GENERATION, COMPRESSION, QUASISTATIC DEFORMATION OF MODEL GRANULAR MATERIALS

grain-level simulations, micromechanical approaches

Role of microscopic model ingredients, definition of relevant variables and control parameters

Jean-Noël ROUX

Laboratoire Navier, Université Paris-Est, France

SCOPE: assembling processes for granular packings, isotropic (or oedometric compression), elastic properties, small to moderate strains in response to deviatoric loads.

Model systems: assemblies of spherical beads (or disks in 2D)

Geometric and micromechanical features

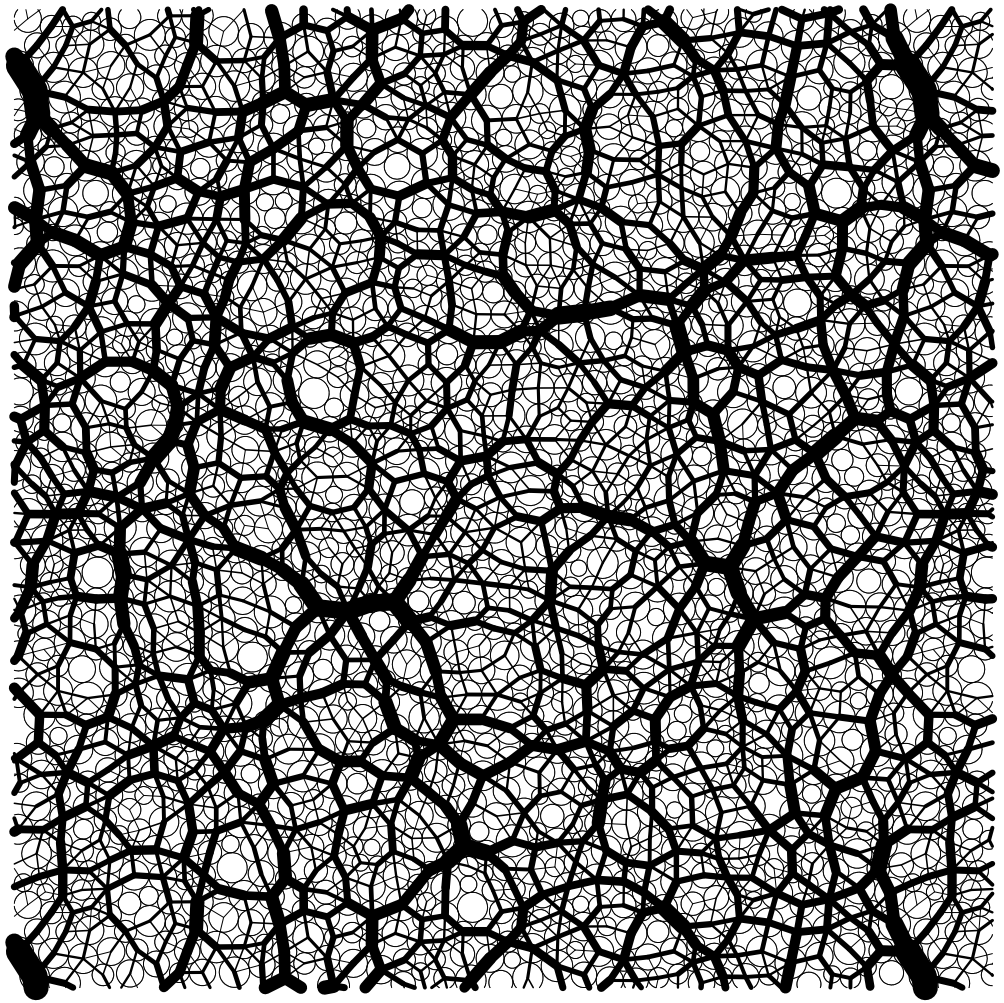

- Note periodic boundary conditions
- Force disorder (force chains, wide force distribution)
- Coordination number $z = 2N_C/N$ (N grains, N_c force-carrying contacts)
- Rattlers – fraction x_0 of grain number – carry no force
- Backbone = force-carrying network of non-rattler grains
- Backbone coordination number = $z^* = \dfrac{z}{1 - x_0}$

Geometric and micromechanical features

- In addition to Φ, z, x_0, force distribution, friction mobilization, introduce fabric or distribution of contact orientations
- Displacement fields also exhibit considerable disorder.

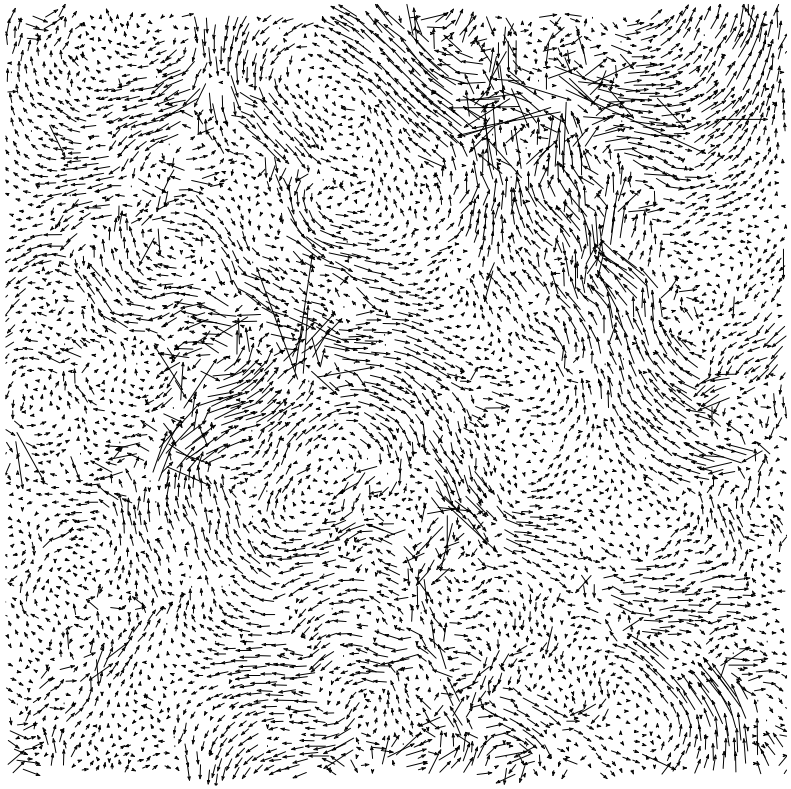

Displacement field $\tilde{\mathbf{u}}_i$ corresponding to small strains ϵ_1, ϵ_2, effect of global strain subtracted:

$$\tilde{\mathbf{u}}_i = \mathbf{u}_i + \underline{\underline{\epsilon}} \cdot \mathbf{r}_i$$

$$\Delta^2 = \frac{1}{n^* ||\underline{\underline{\epsilon}}||^2} \sum_{i=1}^{n^*} ||\tilde{\mathbf{u}}_i||^2$$

to characterize importance of displacement fluctuations. Correlation length ?

CONTACT LAWS

CONTACT LAWS: COULOMB FRICTION

Grains interact mainly via a force at the contact point. Normal component $F_N \geq 0$ is repulsive in the absence of adhesion, and tangential component $\mathbf{F}_T$ satisfies the Coulomb condition

$$\boxed{||\mathbf{F}_T|| \leq \mu F_N}$$

involving the friction coefficient μ.

Little is known in general about μ (depends on surface properties).

In general F_N, $\mathbf{F_T}$ relate to *relative motion* of the rigid bodies (away from contact). Contact laws = solutions to ancillary continuum mechanics problems for 2 infinite half spaces, in contact in a priori unspecified region.

Difficult and sensitive to uncontrolled fine scale features of the material

CONTACT LAWS: NORMAL ELASTICITY

Smooth-shaped, convex grains made of elastic material (E, ν): Hertz law relates F_N to normal contact deflection h.

(2 spheres, diameter a, with $\tilde{E} = E/(1-\nu^2)$) $\boxed{F_N = \frac{\tilde{E}\sqrt{a}}{3} h^{3/2}}$

(Different diameters $\Rightarrow$ use $2a_1a_2/(a_1+a_2)$). Corresponds to stiffness constant

$$\frac{dF_N}{dh} = \boxed{K_N = \frac{\tilde{E}\sqrt{a}}{2} h^{1/2} = \frac{1}{2}(3a)^{1/3}\tilde{E}^{2/3}F_N^{1/3}}$$

Contact region = disk, radius $b = \frac{1}{2}\sqrt{ah}$, normal stress:

$$p(r) = \frac{3F_N}{2\pi b^2}(1 - r^2/b^2)^{1/2}$$

Contact elasticity often modelled as linear, with constant K_N.

$\Rightarrow$ Justification? “Limit of rigid contacts”?

CONTACT LAWS: TANGENTIAL ELASTICITY / FRICTION

Hertz problem + tangential relative displacement, Coulomb condition applied to stress vector (surface traction)

Cattaneo-Mindlin-Deresiewicz problem (see contact mechanics literature)

$\delta \mathbf{u}_T$ = tangential relative displacement $\Rightarrow$ tangential elastic force $\mathbf{F}_T$.

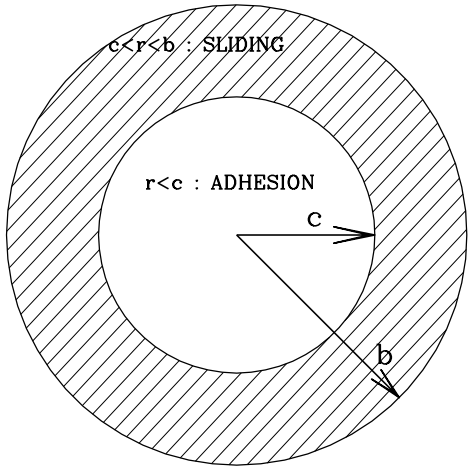

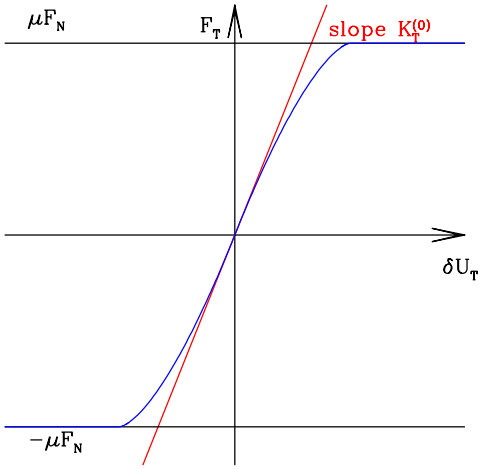

Here $F_N \nearrow$ first, with $\delta u_T = 0$, then δu_T varies at constant F_N.

Tangential stiffness decreases as $\left(1 - \dfrac{||\mathbf{F}_T||}{\mu F_N}\right)^{1/3}$

CONTACT LAWS: TANGENTIAL ELASTICITY / FRICTION

Initial stiffness K_T, as δu_T increases from zero:

$$K_T^{(0)} = \left(\frac{\partial F_T}{\partial(\delta u_T)} \right)_{\delta u_T = 0} = \frac{2-2\nu}{2-\nu} K_N(h)$$

If δu_T decreases, a different unloading path is followed while in an outer annulus $r \geq c'$, $c' > c$ there is slip in the opposite direction, $c < c' \leq r \leq b$

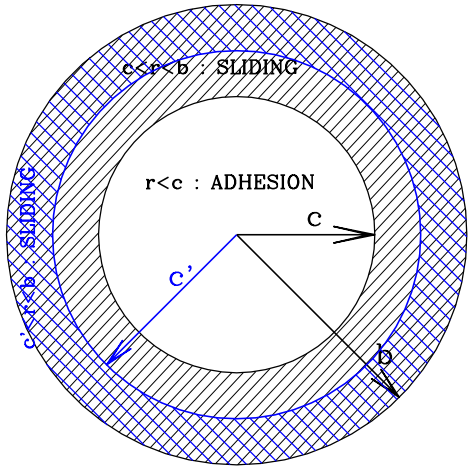

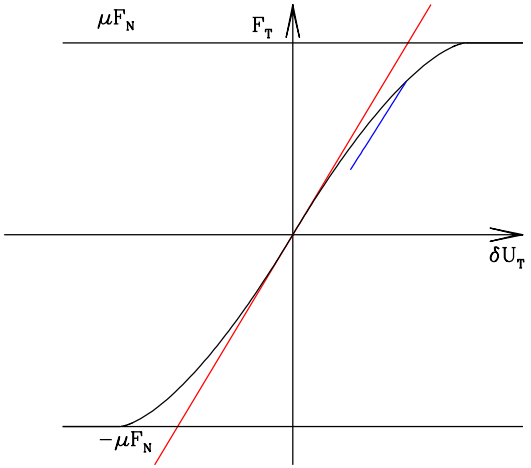

CONTACT LAWS: TANGENTIAL ELASTICITY / FRICTION

Moreover, if both h and δu_T vary simultaneously, stress distributions and forces are path-dependent, even without any local sliding ($\mu = +\infty$) !

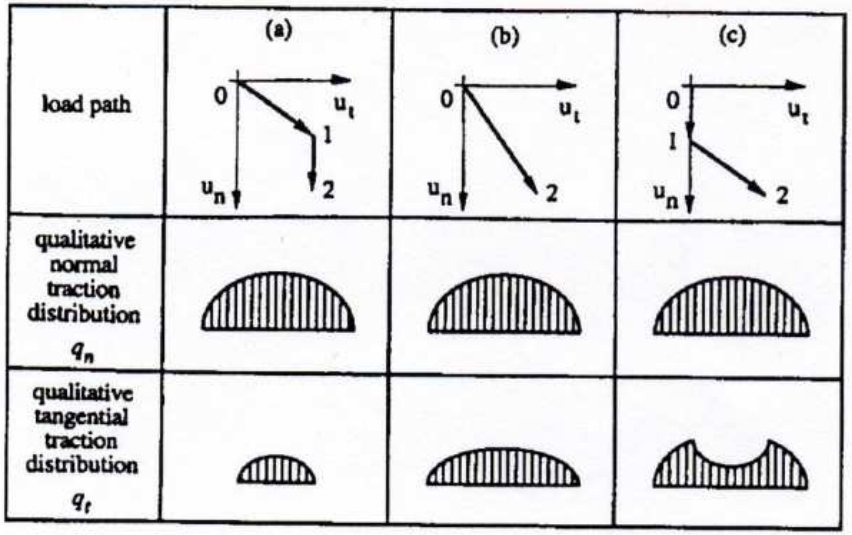

(Elata & Berryman 1996)

$\Rightarrow$ simplification: use tangential stiffness $K_T(h)$ independent of δu_T

Linear tangential elasticity – constant K_T – also often implemented in models.

In calculations, incrementally update $\mathbf{F}_T$ and project back onto circle of radius μF_N in tangential plane if needed

VARIABLE TANGENTIAL STIFFNESS AND ENERGY DISSIPATION

Hysteresis in contact elasticity should imply energy dissipation, not creation!

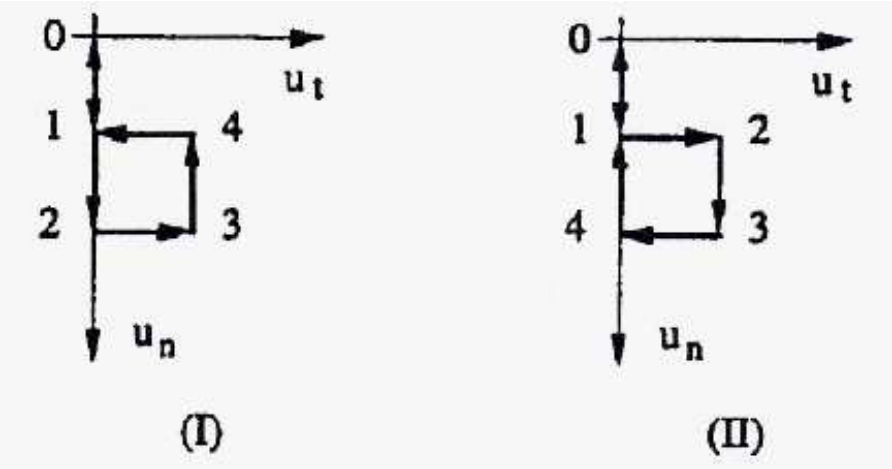

(Elata & Berryman 1996)

$\Rightarrow$ solution: rescale F_T with $K_T(h)$ when it is decreasing, and not when it is increasing (overestimates dissipation)

TANGENTIAL FORCE EVOLUTION IN GENERIC SITUATION

General motion of two contacting grains involves:

1. global motion as one single rigid body
2. relative displacements at contact point (h,$\delta\mathbf{u}_T$) $\rightarrow \Delta F_N$, $\Delta\mathbf{F}_T$
3. rolling (relative rotation about tangential axis)
4. pivoting (relative rotation about normal axis)

How should elastic component $\mathbf{F}_T$ move with the grains (effects of 1, 2, 4) ?
Very little information in the literature!
Should remain tangent and follow rigid-body motion (objectivity)
Possible solution: $\mathbf{F}_T$ follows rolling motion of normal direction $\mathbf{n}$ and rotates about $\mathbf{n}$ with average pivoting rate of both grains

CONTACT FORCES: VISCOUS DISSIPATION

One most often adds viscous terms to elastic components F_N, $\mathbf{F}_T$, opposing relative velocities δV_N, $\delta \mathbf{V}_T$:

$$F_N^v = -\alpha_N \delta V_N \qquad \mathbf{F}_T^v = -\alpha_T \delta \mathbf{V}_T$$

Linear contact elasticity $\Rightarrow$ restitution coefficients e_N, e_T determined by α's. Defining $\zeta = \alpha_N / \alpha_N^c$, critical value $\alpha_N^c = 2\sqrt{m^* K_N}$ with $m^* = \frac{m_1 m_2}{m_1 + m_2}$,

$$e_N = \exp \frac{-\pi \zeta}{\sqrt{1 - \zeta^2}}$$

Choice of $F_N^v = -2\zeta \sqrt{m^* K_N(F_N)} \delta V_N$ with Hertz contacts also yields a velocity-independent restitution coefficient.

In general, viscous forces or restitution coefficients used in simulations do not rely on physical models

Choice: add viscous components to elastic ones and enforce $F_N \geq 0$ in Coulomb condition, or apply inequality to elastic forces only

A PAIR OF GRAINS IN INTERACTIONS : LIST OF PARAMETERS

- Geometry and inertia: diameter a, mass m, moment of inertia, polydispersity parameters
- Contact law:

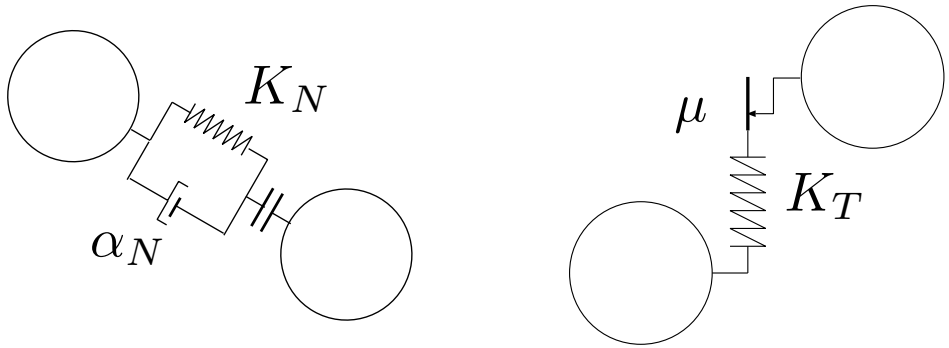

(α_T missing on the figure). $K_{N,T}$ depend on forces (or relative displacements) in general.

- Other possible ingredients (will be mentioned later): resistance to rolling, adhesion
- Many poorly known effects influence dissipation

DIMENSIONLESS CONTROL PARAMETERS

Use of dimensional analysis in order to reduce the number of parameters !
Results in dimensionless form depend on data in dimensionless form
With material parameters + confining pressure P, strain rate $\dot{\epsilon}$,

- Reduced stiffness κ. "Interpenetration" (= contact deflection) $h/a \sim \kappa^{-1}$:
  $\kappa = (\tilde{E}/P)^{2/3}$ for Hertzian contacts in 3D, $K_N/a^{d-2}P$ for linear law with in d dimensions (a = diameter)
  Glass beads, 100 kPa $\Rightarrow \kappa \sim 8400$ if $E = 70$ GPa, $\nu = 0.3$
- Friction coefficient μ (0.2, $\boxed{0.3}$ ... 1 ??)
- K_T/K_N or ν
- Viscous damping level ζ
- Reduced strain rate or inertia number $I = \dot{\epsilon}\sqrt{m/aP}$.
  Quasi-static lab. experiments $\Rightarrow I \sim 10^{-9}$
  Numerically: $I = 10^{-5}$ already very slow and cautious!

Important limits to be investigated

- **Quasistatic limit:** $I \to 0$ (or $\Delta q/p \to 0$ if applied deviator stepwise increased)
  Is I or $\Delta q/p$ small enough ? Do dynamical parameters become irrelevant ? (inertia, viscous forces)
- **Rigid limit:** $\kappa \to +\infty$. Stiffness level irrelevant ? Rigid contact model possible ?
- **Large system limit:** $N \to +\infty$.

Maximum density of identical particles $\Rightarrow$ regular lattices

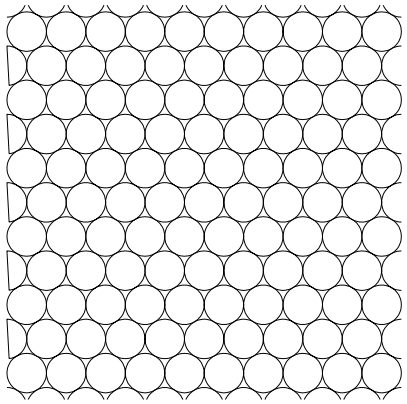

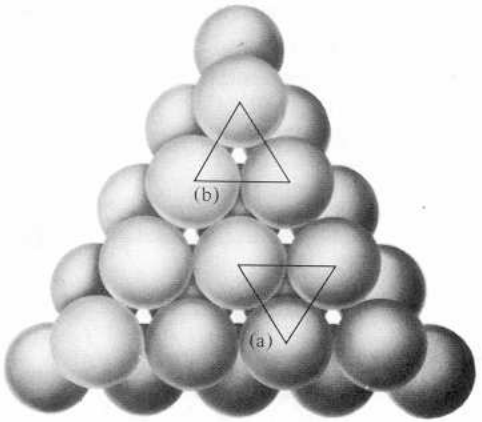

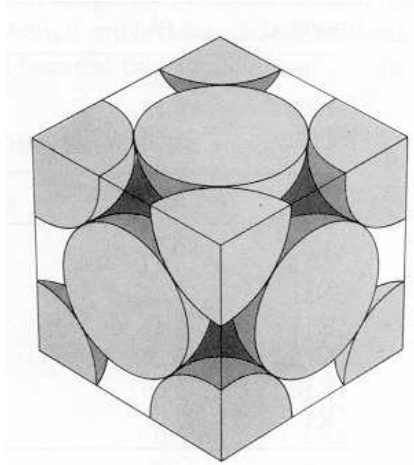

In 2D, $\Phi_{\max} = \dfrac{\pi}{2\sqrt{3}}$.

$z = 6$ on perfect "crystal" lattice, unstable to perturbations

"Crystallisation" is *easy*

En 3D, $\Phi_{max} = \dfrac{\pi}{3\sqrt{2}}$.

$z = 12$ on parfect lattice.

CFC ou hexagonal compact ou hybrides...

"Crystallisation" is *difficult*

In practice avoid equal-sized disks (form spontaneously non-generic, ordered patterns)

Equal-sized spherical balls form disordered assemblies with generic properties

DISORDERED PACK OF IDENTICAL BEADS

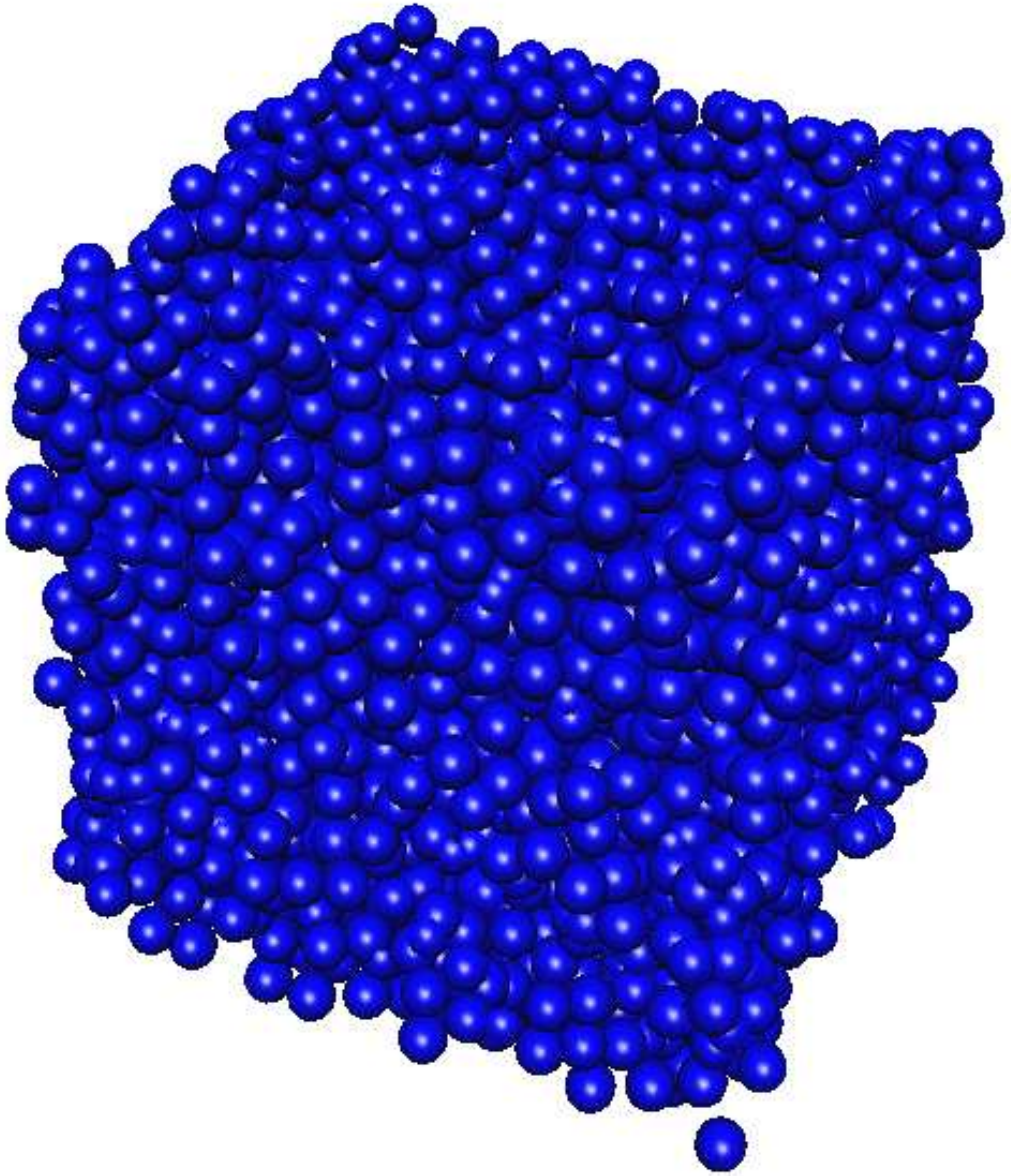

CUT BY A PLANE

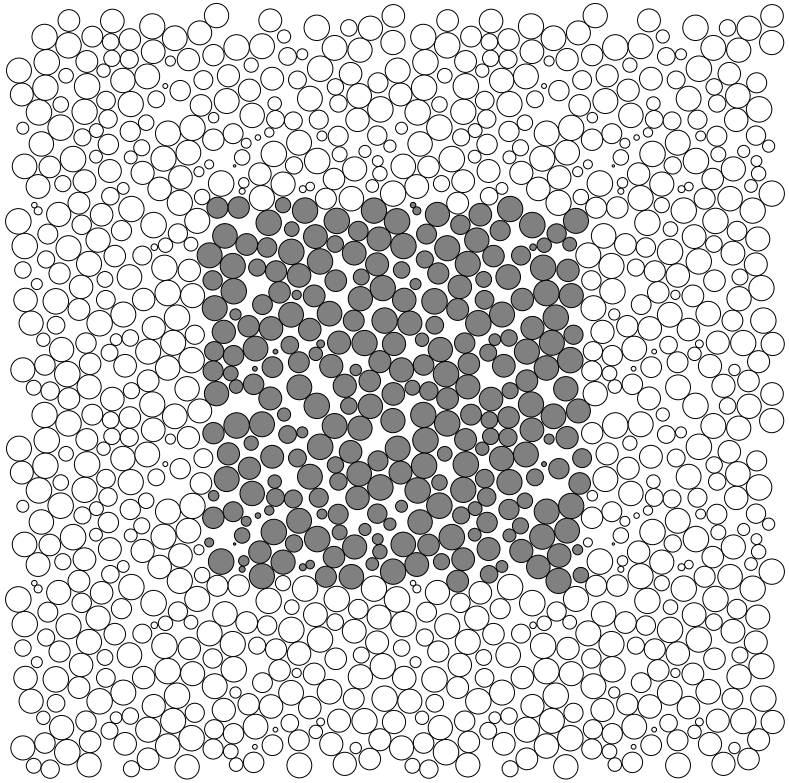

- difficult to measure z directly (even with sophisticated tomographic techniques, cf. Aste *et al.*)
- Here $\Phi \simeq 0.639$ or 0.64 = random close packing (RCP)solid fraction, maximum value for disordered systems. “Order parameters” characterize evolution to crystal patterns on applying repeated shakes or large numbers of shear cycles.

Bounds on coordination numbers

- Upper bound in the rigid limit ($\kappa \to +\infty$) (spheres: $z^* \leq 6$, disks $z^* \leq 4$)
- Lower bound for z^* frictionless spheres or disks (recall $z^* = z/(1-x_0)$), identical
- Lower bound with frictional grains?
  Assume $k = 0$. Then, ($N^* = N(1-x_0)$)

$$\frac{z^* d}{2} - \frac{d(d+1)}{2} + \frac{k}{N^*} \geq \frac{h}{N^*} \geq 0 \quad \Rightarrow \quad \boxed{z^* \geq d+1}.$$

A correction due to mechanisms obtained with spheres:

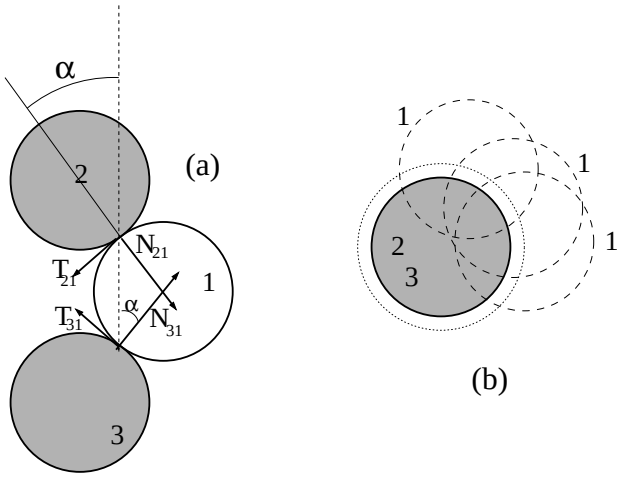

Sphere 1 mobile, 2 and 3 fixed. $h = k = 1$.
If x_2 = fraction of 2-coordinated grains,

$$\boxed{z^* \geq 4 - \frac{2x_2}{3(1-x_0)}}$$

Distribution of contact orientations (fabric)

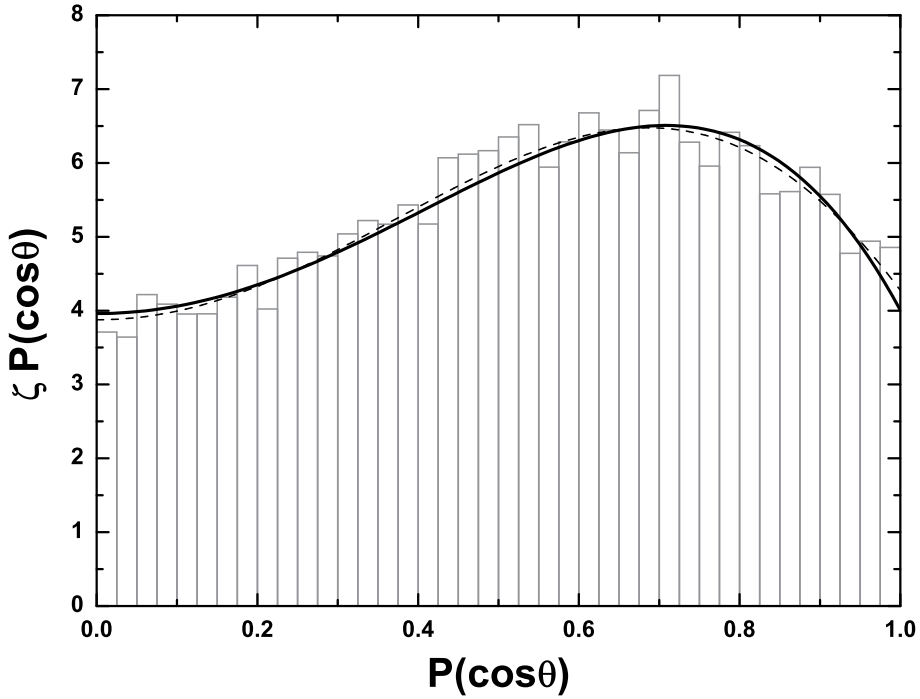

Isotropic $\Rightarrow$ flat distribution

Continuous line = order 4

Dotted line = order 6

$\zeta =$ coordination number

Axisymmetric case (system deposited under gravity). $P(\cos\theta)$ even, restricted to interval $[0, 1]$, expansion in Legendre polynomials:

$$P(\cos\theta) = 1 + b_2 \frac{3\cos^2\theta - 1}{2} + b_4 \frac{35\cos^4\theta - 30\cos^2\theta + 3}{8} + \ldots$$

with

$$b_2 = \frac{15}{2}\left[\langle\cos^2\theta\rangle - \frac{1}{3}\right]; \quad b_4 = \frac{9}{8}\left\{35\left[\langle\cos^4\theta\rangle - \frac{1}{5}\right] - 30\left[\langle\cos^2\theta\rangle - \frac{1}{3}\right]\right\}\ldots$$

Other variables and characteristic features of granular systems in equilibrium

- Probability density function for normal or tangential force values: often measured, described, attempts at predictions... $P(F_N)$ typically flat or slightly increasing below $\langle F_N \rangle$, decreasing (roughly exponentially) above. Shape may be characterized by reduced moments

$$Z(\alpha) = \frac{\langle F_N^\alpha \rangle}{\langle F_N \rangle^\alpha}$$

- Friction mobilization: typically larger for small forces than for large ones
- Connectivity (distribution of number of contacts among grains, x_0, x_2, x_i, $i = 3, 4 \ldots$)
- distribution of interparticle gaps. If cumulated $\Rightarrow z(h)$, coordination number of neighbours at distance $\leq h$
- Force values observed to correlate over distance of several to ~ 10 diameters

Relation between contact forces and stress tensor

Consider a plane surface S, area A cut through granular sample at $z = z_0$, unit normal vector $\mathbf{n}$ (oriented upwards, $z \nearrow$).

$\mathbf{J}(z_0)$ = momentum transferred from lower part $z < z_0$ to upper part $z > z_0$ per unit time = (kinetic contribution) + (contribution of forces, $\mathbf{J}_f(z_0)$).

In equilibrium, $\mathbf{J} = \mathbf{J}_f$

Then $\mathbf{J}(z_0) = A\underline{\underline{\sigma}} \cdot \mathbf{n}$ or, for coordinate α, $J^\alpha(z_0) = A\sigma_{\alpha z}$

$$\mathbf{J}(z_0) = \sum_{i \mid z_i < z_0,\, j \mid z_j > z_0} \mathbf{F}_{ij}$$

Macroscopic stresses vary on scale $L \gg a \Rightarrow$ average over position z_0 ($a \ll l \ll L$)

$$A\underline{\underline{\sigma}} \cdot \mathbf{n} = \frac{1}{l}\int_{z_0-l/2}^{z_0+l/2} \mathbf{J}(z)dz$$

$$= \frac{1}{2l} \sum_{|z_i-z_0|<l/2, |z_j-z_0|<l/2} \mathbf{F}_{ij}(z_j - z_i)$$

$$= \frac{1}{2l} \sum_{|z_i-z_0|<l/2, |z_j-z_0|<l/2} \mathbf{F}_{ij}\left[(\mathbf{r}_j - \mathbf{r}_i)\cdot \mathbf{n}\right]$$

whence for a sample of volume V in uniform state of stress:

$$\underline{\underline{\sigma}} = \frac{1}{V}\sum_{i=1}^{N} \frac{1}{2}\left(\sum_{j,\, j\neq i} \mathbf{F}_{ij} \otimes \mathbf{r}_{ij}\right),$$

with $\mathbf{r}_{ij} = \mathbf{r}_j - \mathbf{r}_i$, or

$$\underline{\underline{\sigma}} = \frac{1}{V} \sum_{1\leq i<j\leq N} \mathbf{F}_{ij} \otimes \mathbf{r}_{ij}.$$

$$\sigma_{\alpha\beta} = \frac{1}{V}\sum_{i<j} F_{ij}^{(\alpha)} r_{ij}^{(\beta)}$$

Average contact force and pressure

With spherical grains $\mathbf{r}_{ij}$ and $\mathbf{n}_{ij}$ are parallel. In dimension $d = 3$ or 2

$$P = \frac{1}{d}\sum_{i=1}^{d}\sigma_{ii} = \frac{1}{dV}\sum_{i<j}F_{ij}^{N}(R_i + R_j)$$

N_c contacts, grain diameter a $\Rightarrow P = \dfrac{aN_c}{3V}\langle F^N\rangle$

Contact density N_c/V also writes $z\Phi/(2v)$ with $v = \pi a^d/(2d$=volume of one grain.

Therefore,

$$\langle F^N\rangle = \frac{\pi a^{d-1}}{z\Phi}P.$$

With different diameters, assuming $\langle F_{ij}^{N}(R_i + R_j)\rangle = \langle F^N\rangle\langle a\rangle$,

$$P = \frac{\pi\langle a^d\rangle}{z\Phi F_N\langle a\rangle}.$$

Accurate formula for moderate polydispersity (say, diameter ratio below ~ 3)

Some useful quantities in packs of Hertzian beads

- Typical contact deflection

$$\frac{\langle h^{3/2}\rangle^{2/3}}{a} = \left(\frac{3\pi P}{z\Phi\tilde{E}}\right)^{2/3} = \left(\frac{3\pi}{z\Phi}\right)^{2/3}\kappa^{-1}$$

- Average contact stiffness

$$\langle K_N\rangle = \frac{3^{1/3}}{2}\tilde{E}^{2/3}a^{1/3}Z(1/3)\langle F_N\rangle^{1/3} = \frac{1}{2}\tilde{E}^{2/3}P^{1/3}\left(\frac{3\pi}{z\Phi}\right)^{1/3}a$$

- Maximum pressure within contact transmitting normal force F_N

$$\frac{p_{\max}}{\tilde{E}} = \frac{2\times 3^{1/3}}{\pi^{2/3}(z\Phi)^{1/3}}\left(\frac{F_N}{\langle F_N\rangle}\right)^{1/3}\kappa^{-1/2}$$

- Maximum shear stress near contact transmitting normal force F_N

$$\frac{\tau_{\max}}{\tilde{E}} \simeq 0.31\frac{p_{\max}}{\tilde{E}} \quad (\text{if } \nu = 0.3)$$

Material elastic moduli, amounts of damage, etc... independent of a

ASSEMBLING PROCEDURES

Numerical assembling procedures (no cohesion)

1. Idealised methods, to explore range of possible configurations, all perfectly isotropic
2. Simulation of one laboratory method: controlled pluviation
3. Other deposition processes under gravity

Numerical preparation of isotropic configurations (no cohesion)

2 procedures:

- Isotropic compression of a "granular gas" (no contact , solid fraction $\Phi = 0.45$) Apply $P = 10$kPa, request $I \leq 10^{-4}$, until equilibrium $\kappa = 39000$ for GB. Both Φ and coordination number z decrease as $\mu \nearrow$. One may use $\mu_0 < \mu$.
  - Classical trick to get a dense state: use $\mu_0 = 0$ (state A).
  - $\mu_0 = \mu \Rightarrow$ looser state D
  - $\mu_0 = 0.02$: imperfect lubrication, B
- Compaction *via* vibration $\Rightarrow$ different dense states, C. Dilate configuration A (coord. $\times\lambda > 1$), then vibrate (kinetic energy) and then compact ($\mu = 0.3$).

Ideal, isotropic assembling procedures (our results with I. Agnolin)

Here $\mu = 0.3$ Friction mobilisation:

$$M_1 = \langle \frac{F_T}{F_N} \rangle \quad \text{for } F_N > \langle F_N \rangle \, ; \quad M_2 = \langle \frac{F_T}{F_N} \rangle \quad \text{for } F_N \leq \langle F_N \rangle$$

Procedure	Φ	z^*	x_0 (%)	x_2 (%)	Z(2)	M_1	M_2
A	0.637	6.074	1.3	0	1.53	0	0
B ($\mu_0 = 0.02$)	0.6271	5.80	1.65	$\sim 10^{-4}$	1.52	0.016	0.018
C ($\lambda = 1.005$)	0.635	4.56	13.3	2.64	1.65	0.135	0.181
D	0.593	4.546	11.1	2.39	1.58	0.160	0.217

$\Phi_C > \Phi_B$ but $z_C^* < z_B^*$. *Φ and z^* independent for isotropic states*

vibration procedure $\rightarrow$ low coordination in final equilibrated state

The random close packing state (RCP , $\Phi^* \simeq 0.639$)

- frictionless contacts in assembling stage $\Rightarrow$ apparently **unique** (isotropic) state independent on dynamical parameters and process, if fast enough
- enduring agitation at $0.5 \leq \Phi = 0.5 \leq 0.6 \rightarrow$ partial crystallisation
- stable equilibrium of rigid, frictionless objects = local density maximum in configuration space. Thus

  To increase density, reduce or circumvent friction
- $z^* = z/(1 - x_0)$ equal to 6 for spheres in the rigid limit $\kappa \rightarrow +\infty$ (consequence of isostaticity)

RCP= frictionless equilibrium state, for $\kappa \rightarrow \infty$, isotropic, assembled on minimising crystallisation

Laboratory assembling processes are rather fast (similar time scales as numerical compression)

The random close packing state

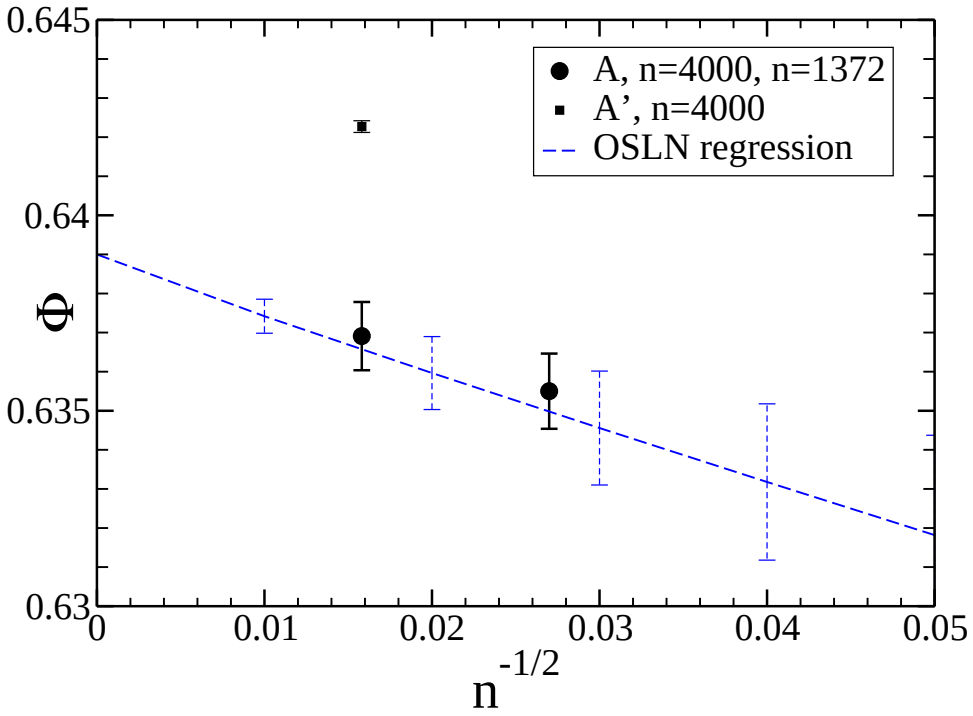

A = fast compression, frictionless. A' = longer agitation (Lubachevsky-Stillinger algorithm)

OSLN = results by O'Hern *et al.*, 2003, different simulation method, Dots = DEM preparation.

A' more ordered than A.

With bidisperse systems: separation rather than crystallisation.

Geometry of sphere assemblies: interstices

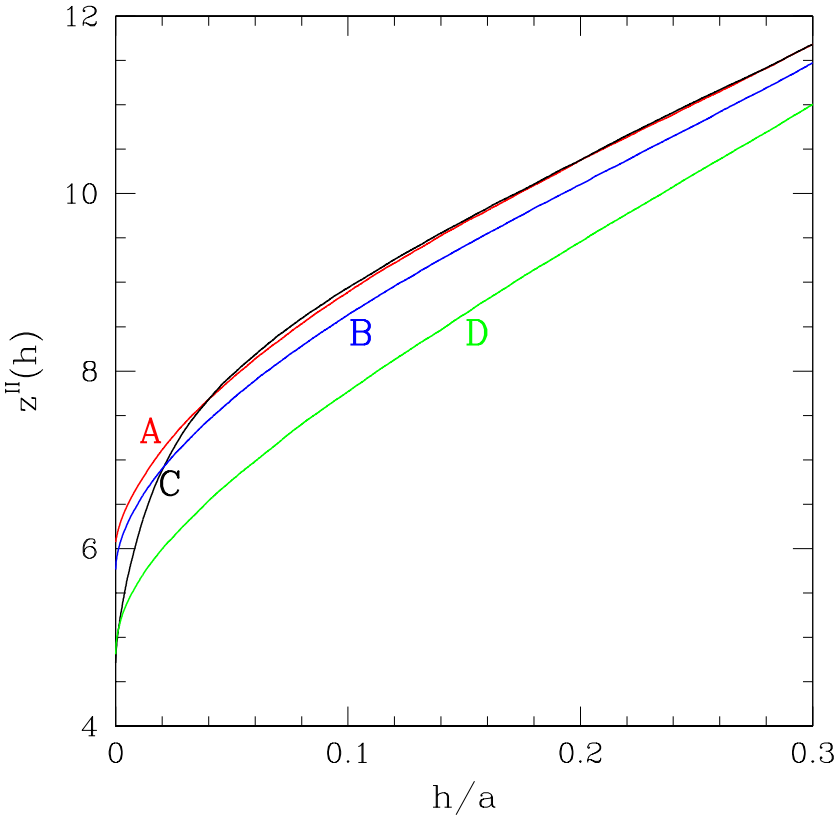

Gap-dependent coordination number: number of neighbors at distance $\leq h$. Here rattlers have been "stuck" to backbone to get a fully defined packing geometry

Results for $h/a \leq 0.04$ not determined by density, still inaccessible to direct measurements (X-ray tomography, Aste *et al.* 2004, 2005 : accuracy of $\sim 0.05 \times a$)

“Ideal” isotropic assemblies

- No dependence on dynamical parameters (if compression is slow enough, say $I \leq 10^{-4}$)
- Definition of random close packing
- Enduring agitation induce ordering or separation by size
- Coordination number and density can vary independently – undetectable in 3D systems by direct visualisation

Controlled pluviation : principle, control parameters

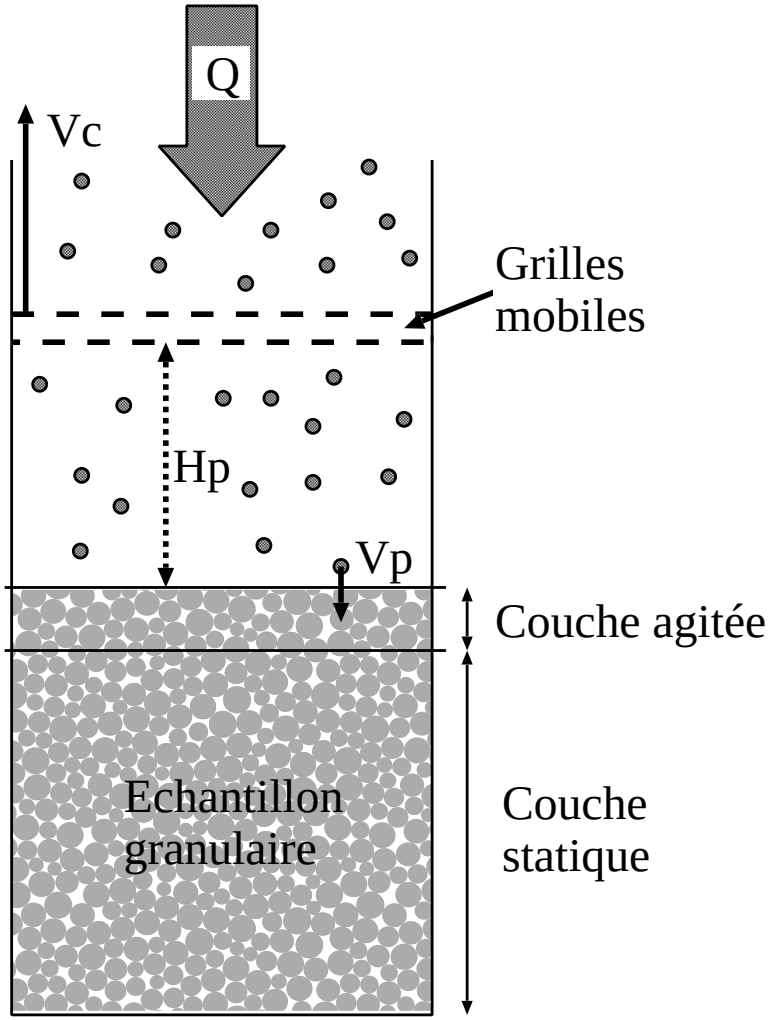

- Constant height of free fall H_p $\Rightarrow$ dimensionless ratio

$$H_p^* = \frac{H_p}{a}$$

- mass flow rate per unit area Q, controlled from upper reservoir outlet

  $\Rightarrow$ reduced flow rate

$$Q^* = \frac{Q}{\rho_p \sqrt{ag}}$$

- agitation in superficial layer, approach to equilibrium below
- Final density $\nearrow$ as H_p^* $\nearrow$ and as Q^* $\searrow$

Distribution of contact orientations (fabric)

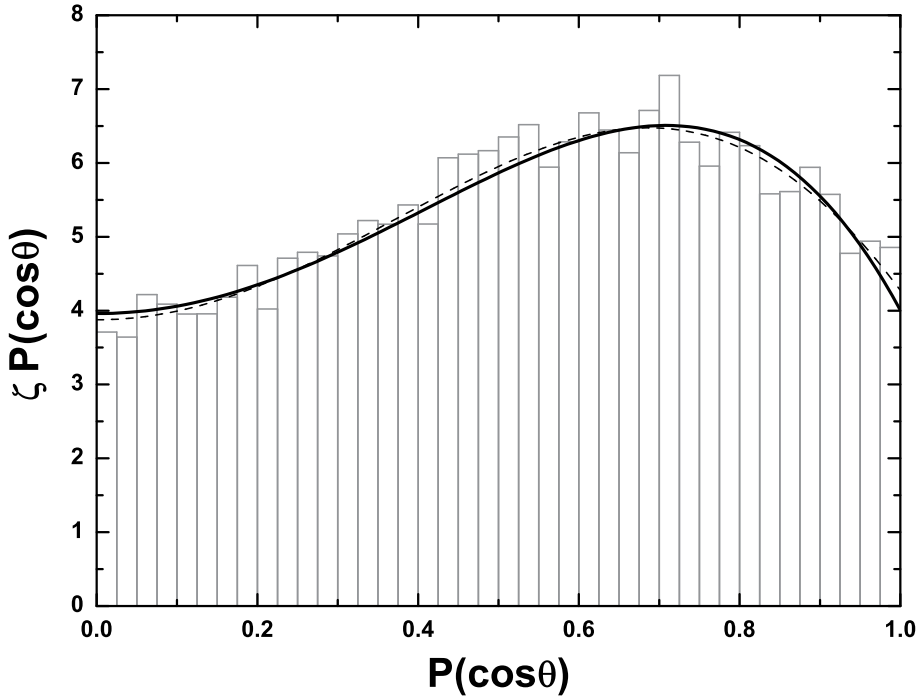

Isotropic $\Rightarrow$ flat distribution

Continuous line = order 4

Dotted line = order 6

$\zeta =$ coordination number

Axisymmetric case (system deposited under gravity). $P(\cos\theta)$ even, restricted to interval $[0, 1]$, expansion in Legendre polynomials:

$$P(\cos\theta) = 1 + b_2 \frac{3\cos^2\theta - 1}{2} + b_4 \frac{35\cos^4\theta - 30\cos^2\theta + 3}{8} + \ldots$$

with

$$b_2 = \frac{15}{2}\left[\langle\cos^2\theta\rangle - \frac{1}{3}\right]; \quad b_4 = \frac{9}{8}\left\{35\left[\langle\cos^4\theta\rangle - \frac{1}{5}\right] - 30\left[\langle\cos^2\theta\rangle - \frac{1}{3}\right]\right\}\ldots$$

Simulating the pluviation process: results

- anisotropic states, characterised by distribution of $\cos\theta$, $\theta =$ angle between normal to contact and vertical direction
- Homogeneity: same state, apart from stress level, except near bottom or top
  Wrong if H_p not constant !
- Under agitated upper layer, nearly quasistatic oedometric compression
- Influence of viscous damping (bad news !)
- Difficult to compare with experiment (damping + shape/size of beads) $\Rightarrow$ compare mechanical properties !
- Coordination and fabric conserved on isotropically compressing
- Moderate fabric anisotropy and rather large coordination number (closer to A than C in dense states) with “reasonable” choices of damping parameters

Final state (simulations).

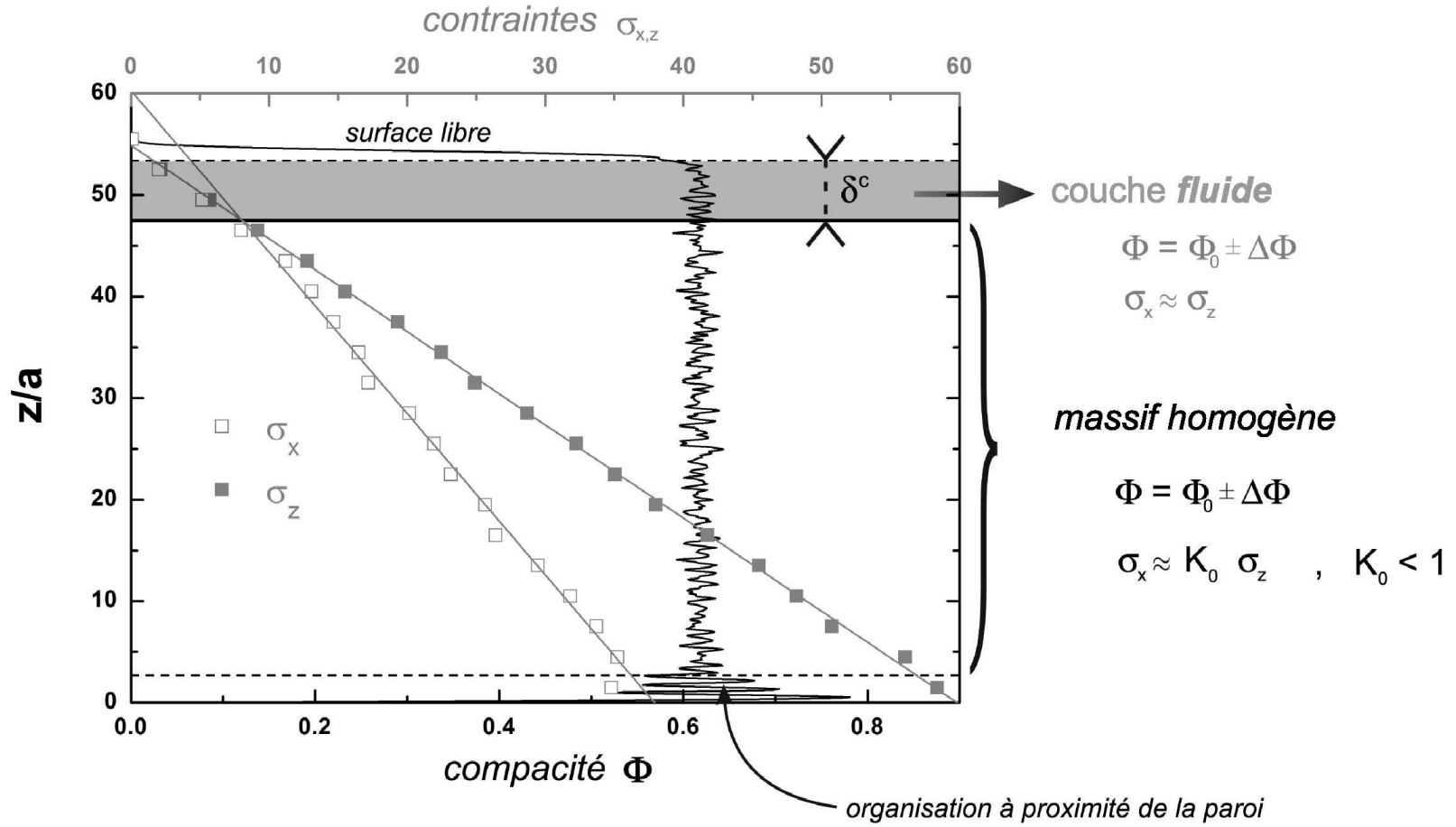

Density is fixed once material is buried under surface, “fluid” layer.

σ_h/σ_v decreases from 1 (fluid) to $K_0 < 1$. Fabric anisotropy as shown previously

numerical results: S. Emam

Less controlled pluviation

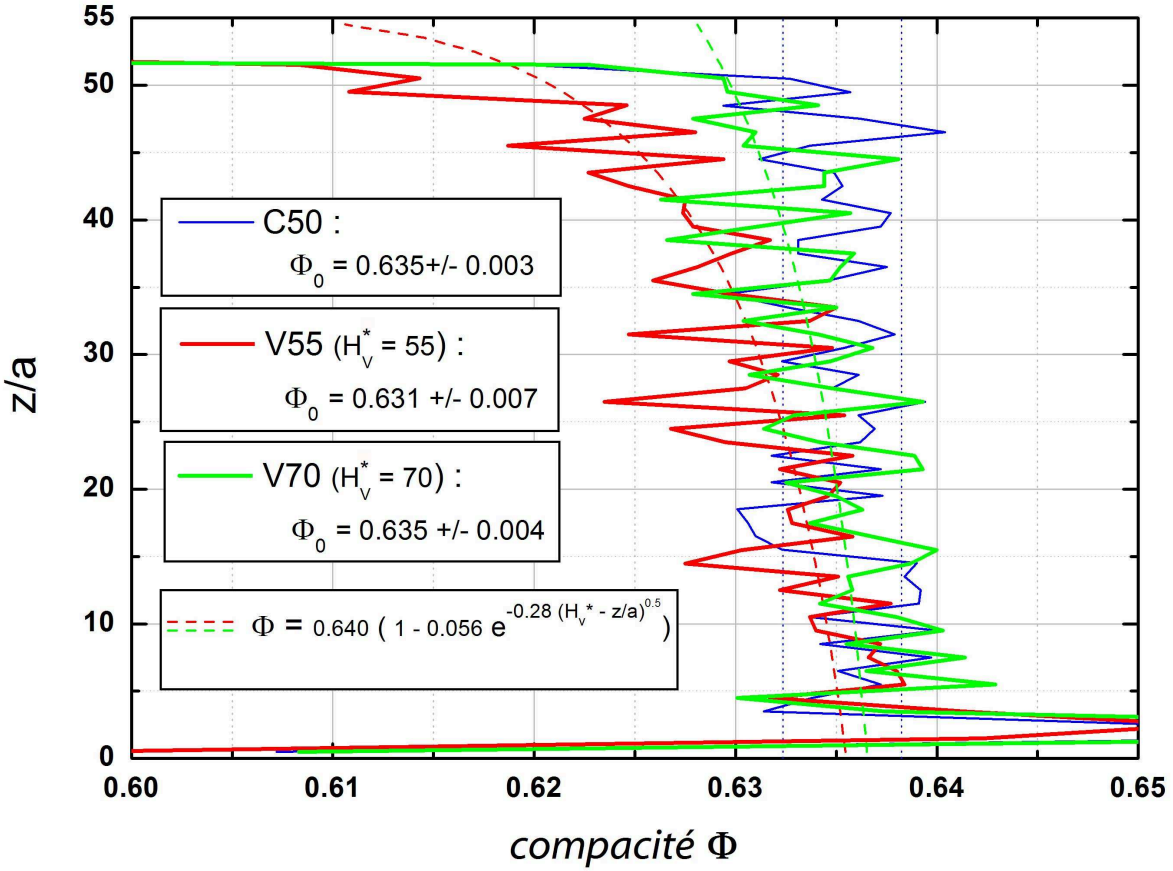

Drop the grains from fixed height (red) $\Rightarrow$ larger density at bottom, where H_p^* is larger.

Dotted curve = pluviation results with varying H_p^*

Blue = controlled pluviation result

Fabric in 2D

Angular distribution of normal vector orientation at contacts $p(\theta)$ is π-periodic

If system is symmetric about axis $\theta = 0$, $p(\theta)$ is an even function, whence a Fourier expansion as

$$p(\theta) = \frac{1}{2\pi}\left(1 + \sum_{k\geq 1} a_k \cos 2k\theta\right)$$

Coefficients are given by $a_k = 2\langle \cos 2k\theta \rangle$.

$$\langle \mathbf{n} \otimes \mathbf{n} \rangle = \begin{bmatrix} \frac{1}{2} + \frac{a_2}{4} & 0 \\ 0 & \frac{1}{2} - \frac{a_2}{4} \end{bmatrix}$$

Some results on 2D granular layers under gravity (G. Combe)

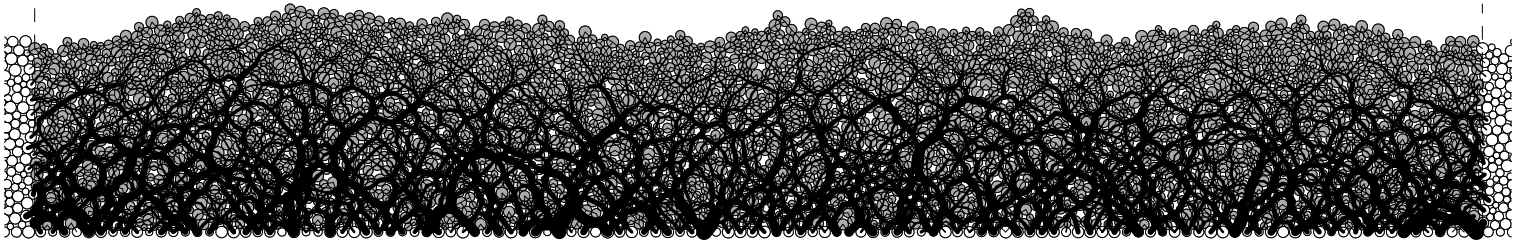

Fabric in grain by grain deposition (left) versus bulk dumping (right)

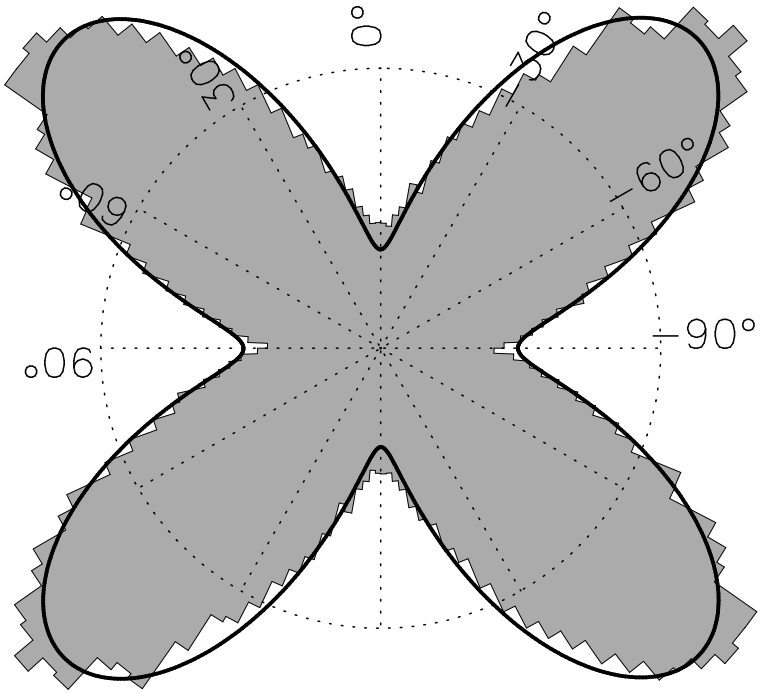

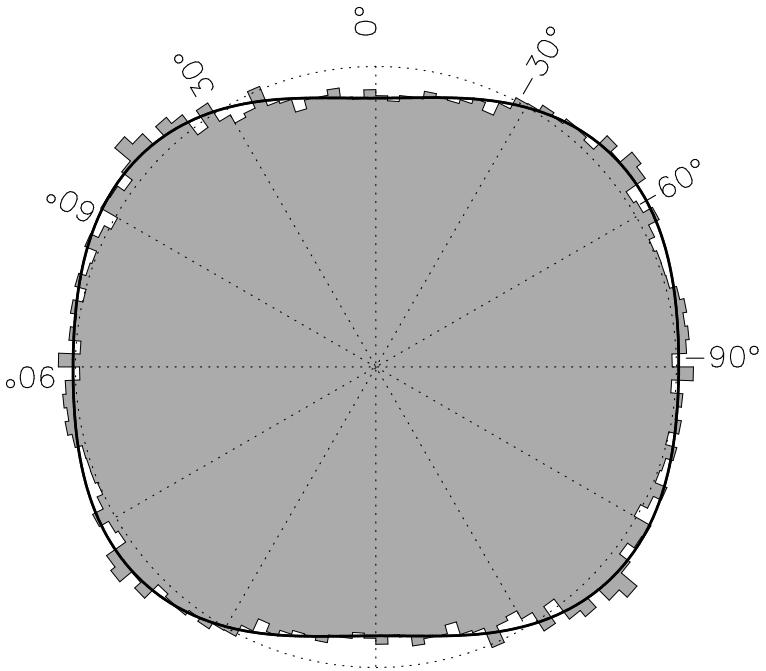

Extreme fabric anisotropy, fitted with 2 coefficients (a_2 and a_4)

Some results on 2D granular layers under gravity

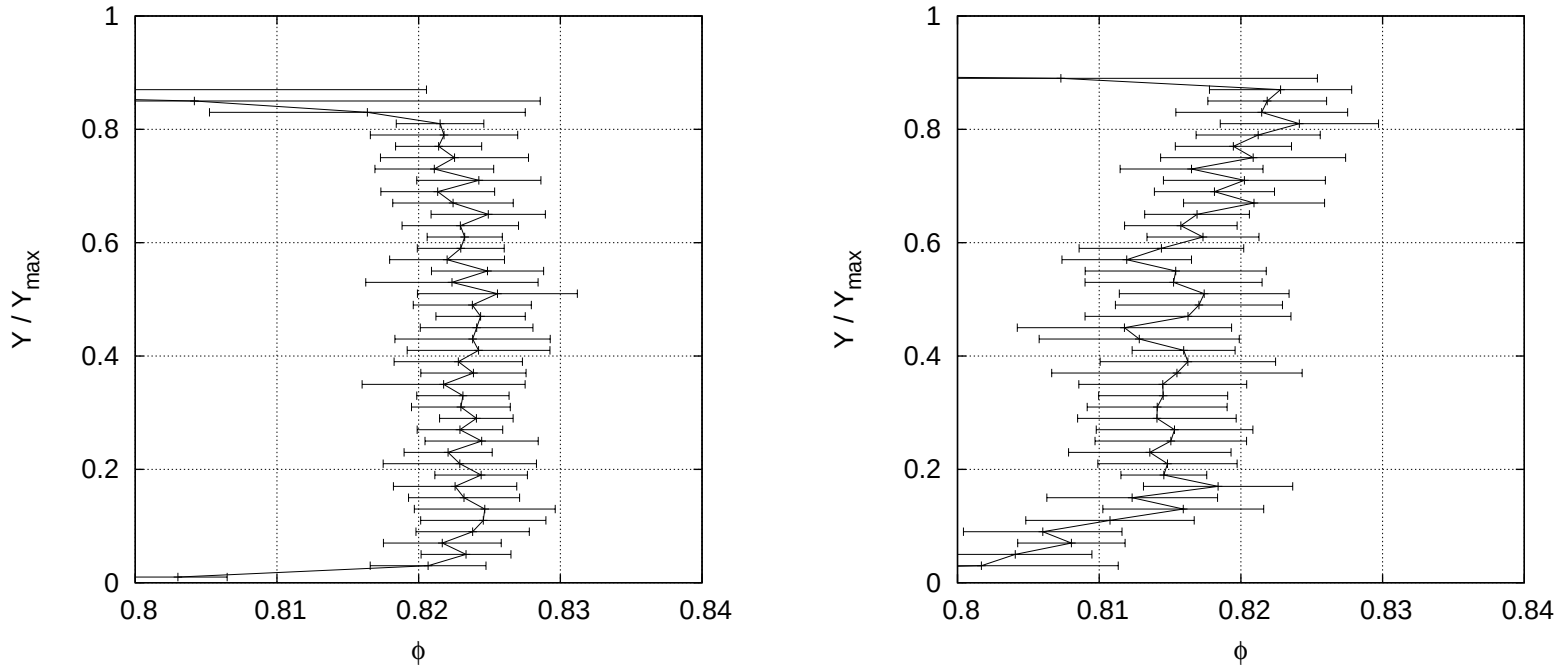

Unlike grainwise deposition (left), bulk dumping (right) results in inhomogeneous solid fraction. Wave propagates upwards after pack hits substrate.

Some results on model cohesive powders (2D)

(coll. F. Gilabert & A. Castellanos, Seville)

Additional ingredients in contact law: Adhesion...

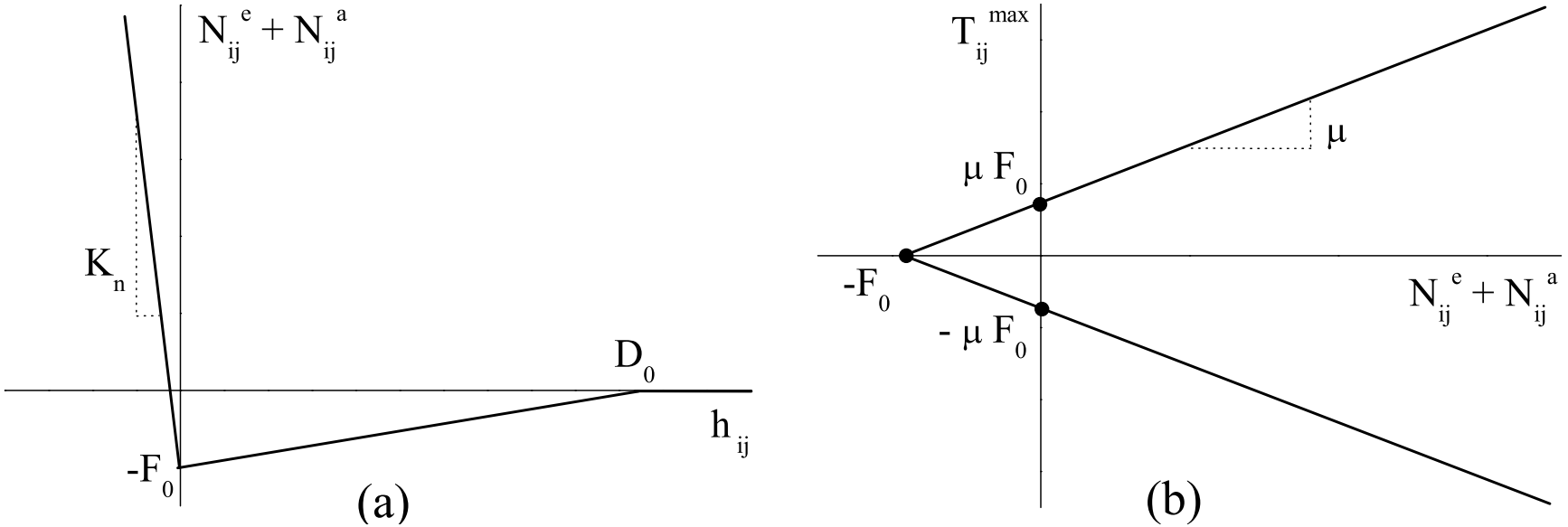

... and (possibly) rolling resistance: F_T, Γ at contact limited by μN^e, resp. $\mu_r N^e$

$\Rightarrow$ a contact with deflection h_0 such that $N = N_e - F_0 = 0$ can resist tangential relative displacement and rolling $\Rightarrow$ enhanced effects of friction and rolling friction

Physically, μ_r (length) is of order l (distance between asperities)

Effects of cohesion

- Let grains "stick" to one another (*e.g.*, ballistic aggregation), until a macroscopic aggregate has formed, then apply external pressure $\Rightarrow$ very loose states
- Geometry studied in colloid aggregation models... now one may study **mechanics** as well!
- importance of irreversible compaction ("consolidation curve") under *isotropic* loads
- Behaviour ruled by reduced pressure $\boxed{P^* = \dfrac{a^{d-1}P}{F_0}}$. Cohesion dominates for $P^* \ll 1$, external pressure dominates for $P^* \gg 1$ (similar, then, to cohesionless case)

Preparation method: aggregation versus compression

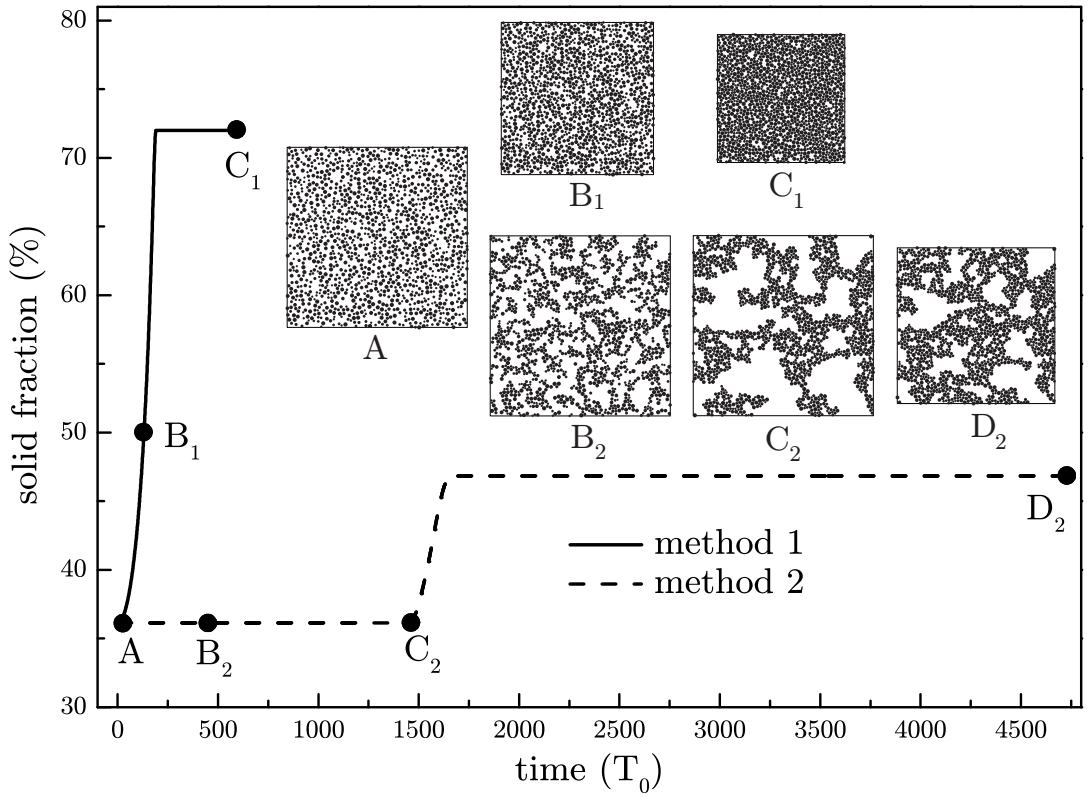

(1) Direct compression of isolated grains $\rightarrow$ dense configuration

(2) Aggregation first, until only one cluster is present, then compression to $P^* = 0.01 \Rightarrow$ looser state.

$T_0 = \sqrt{ma^2/F_0}$. Note long equilibration times.

Loose structure under $P^* \ll 1$

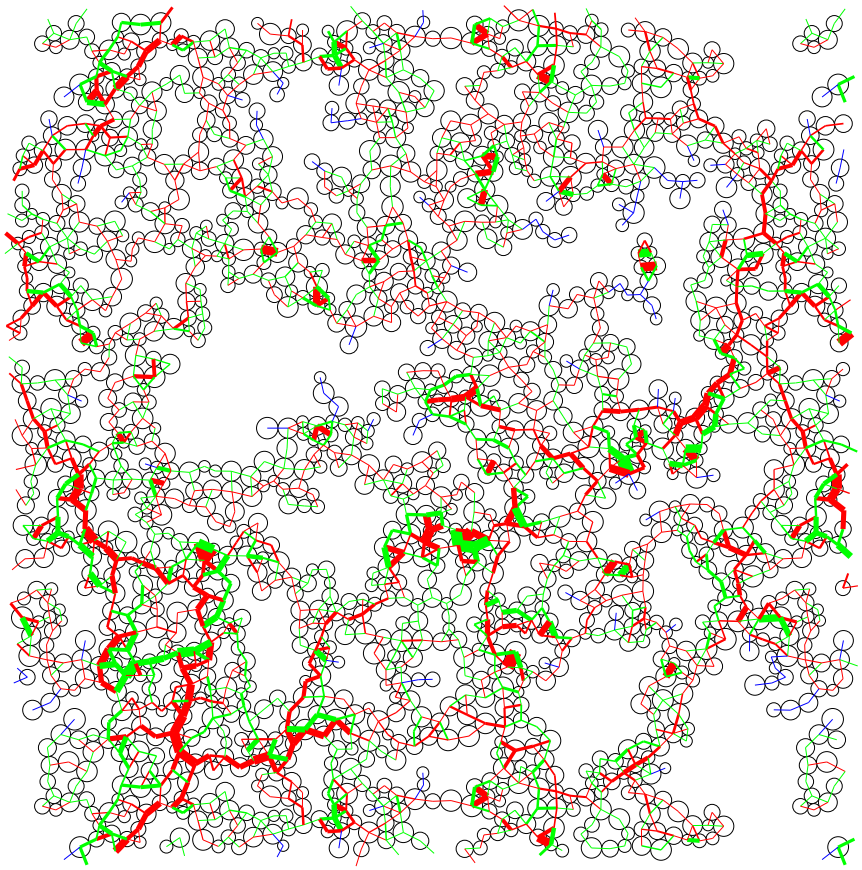

Repulsive and attractive forces of order F_0 nearly compensate.

Blue lines, grey disks = unstressed regions

Fractal structure below length ("blob size") $\xi \sim 5$ to $10a$

Fractal dimension of ballistic aggregation process ($d_F \simeq 1.55$) with small RR, different without RR.

Effect of small RR

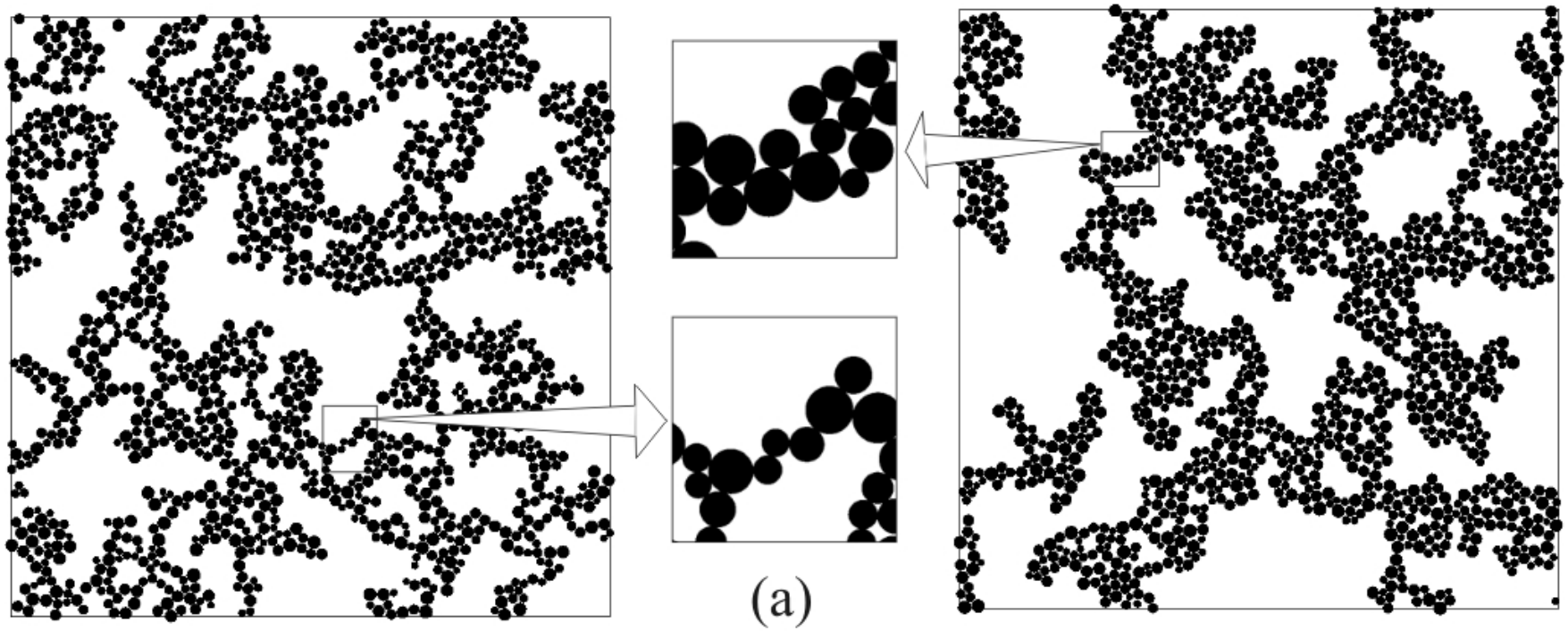

With RR (left) thinner “arms”, smaller d_F

In ballistic aggregation aggregates are undeformable solids, and form without loops $\Rightarrow z = 2$. With RR the degree of force indeterminacy is the number of independent loops of the contact network.

Force networks: small RR, effect of initial energy

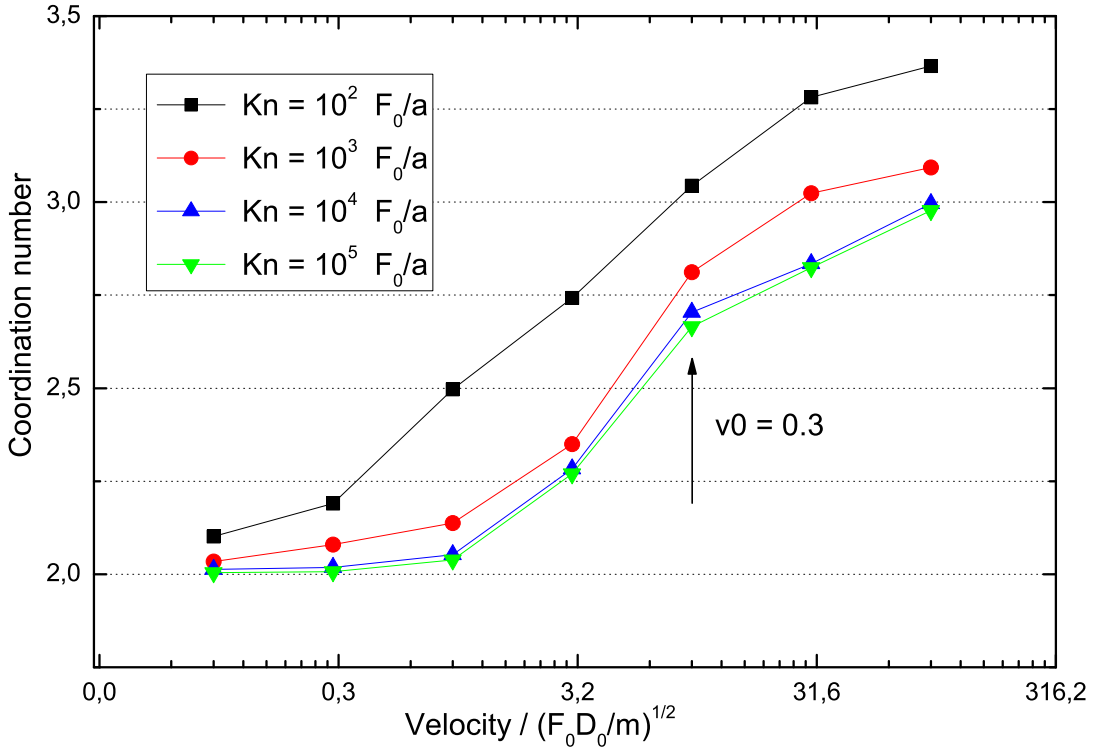

$l = a$ or $\mu_r = 0.5a$

Compare initial agitation velocity V_0 to "escape velocity" out of attractive potential

Geometric rule retrieved only for slow initial velocities in the limit of rigid contacts

μ, μ_r irrelevant for initial assembling phase in that limit

Some conclusions on preparation process of solid granular samples

- Density alone not enough to classify packings: coordination number may change a lot for dense samples Extreme cases obtained with (idealised) lubrication and with (idealised) vibration
- Compacting = avoiding the effects of friction
- Moderate anisotropy in simulations of pluviation (coordination similar to partially lubricated case)
- Cohesive systems exhibit a much wider variety of structures, form loose structures with different degrees of branching... Assembling stage bound to depend on effects of surrounding fluid in practice